Supplementary information for

Yolk-albumen-shell structure of mixed Ni-Co oxide with ultrathin carbon shell for high-sensitivity glucose sensors

Xuan Zhang[1, 2], Yawei Zhang[1], Maowen Xu[1]*, Wei Guo[2], Kai Wan[2], Ting Zhang[3], Jordi Arbiol[3,4]*, Yong-Qing Zhao[5], Cai-Ling Xu[5], Jan Fransaer[2]*

[1] *Department of Materials Engineering, KU Leuven, Leuven 3001, Belgium. E-mail: jan.fransaer@ kuleuven.be;*

[2] *Key Laboratory of Luminescent and Real-Time Analytical Chemistry (Southwest University), Ministry of Education, School of Materials and Energy, Southwest University, Chongqing 400715, PR China. E-mail: xumaowen@swu.edu.cn;*

[3] *Catalan Institute of Nanoscience and Nanotechnology (ICN2), CSIC and BIST, Campus UAB, Bellaterra, 08193 Barcelona, Catalonia, Spain. E-mail: arbiol@icrea.cat*

[4] *ICREA, Pg. Lluís Companys 23, 08010 Barcelona, Catalonia, Spain*

[5] *State Key Laboratory of Applied Organic Chemistry, Key Laboratory of Nonferrous Metal Chemistry and Resources Utilization of Gansu Province, Laboratory of Special Function Materials and Structure Design of the Ministry of Education, College of Chemistry and Chemical Engineering, Lanzhou University, Lanzhou, 730000, China*

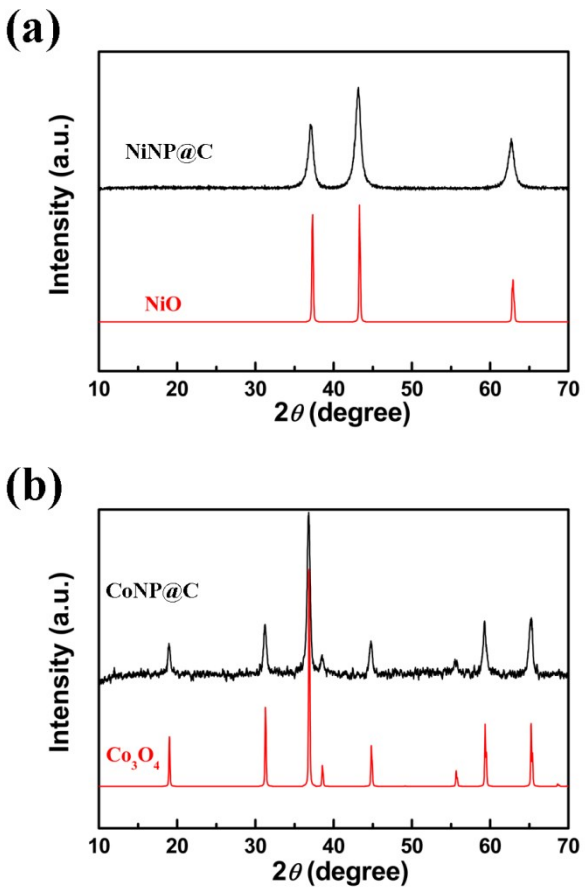

Figure S1. XRD pattern of (a) NiNP@C and (b) CoNP@C. (using Cu K_α radiation with wave length λ = 0.15405 nm and Ni filter with a step size of 0.02°)

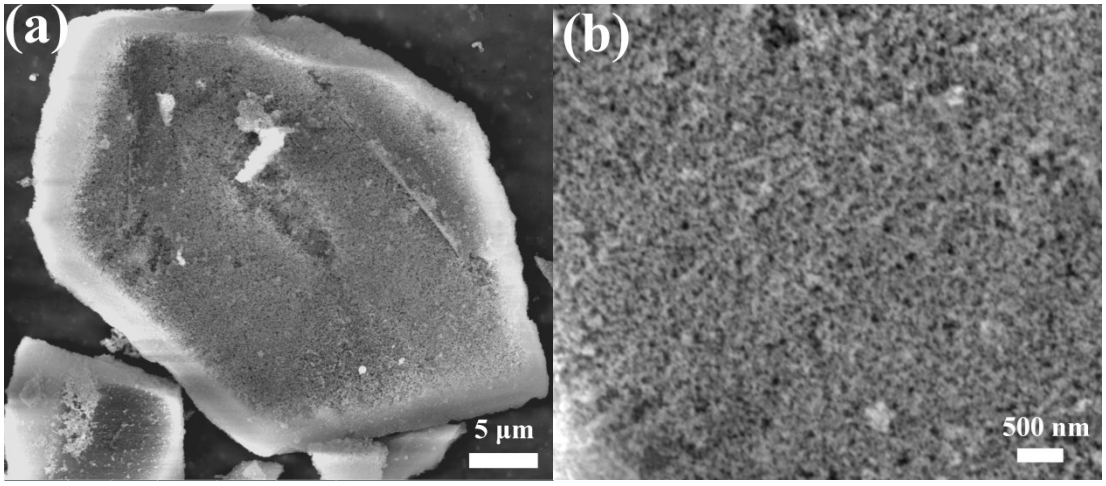

Figure S2. SEM images (at an acceleration voltage of 15 kV) of NiNP@C

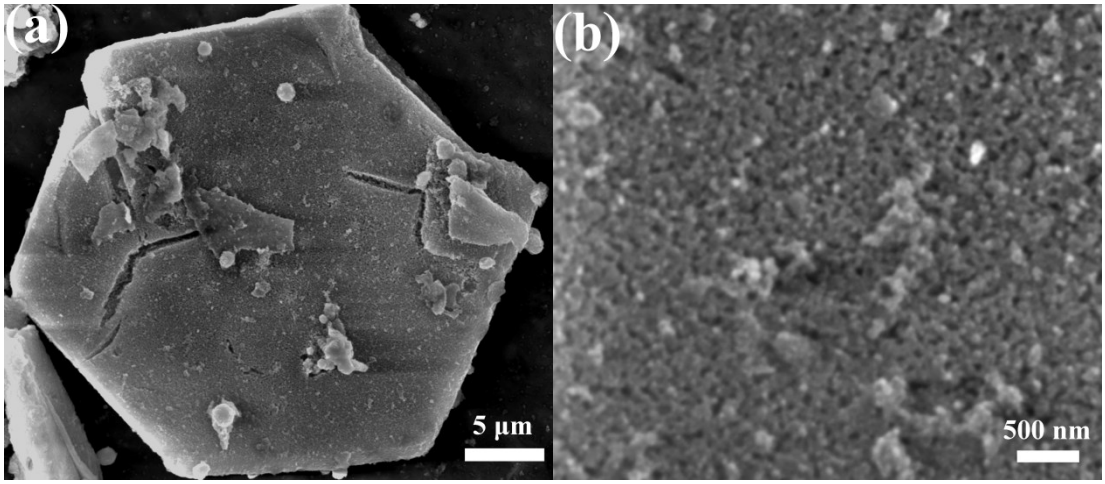

Figure S3. SEM images (at an acceleration voltage of 15 kV) of YASNiCo@C

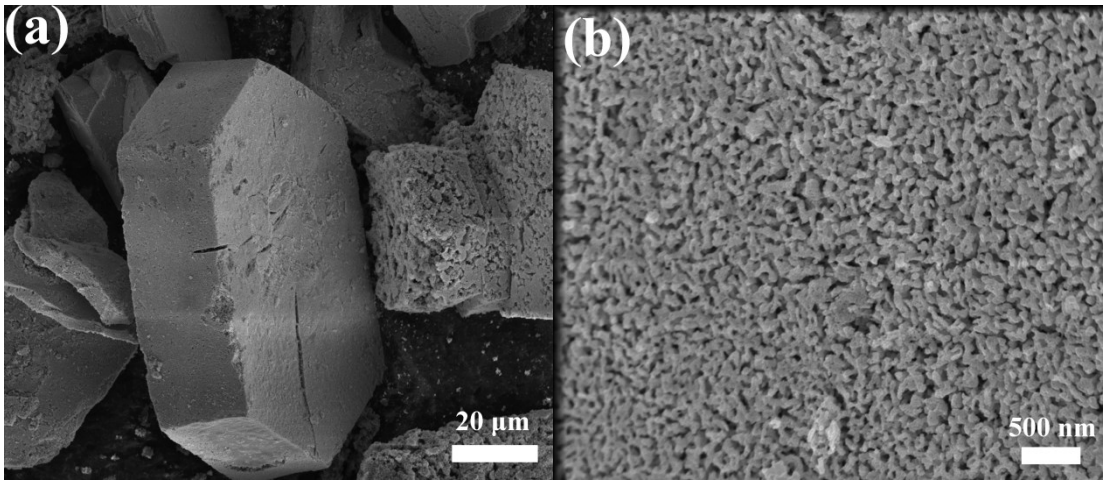

Figure S4. SEM images (at an acceleration voltage of 15 kV) of CoNP@C

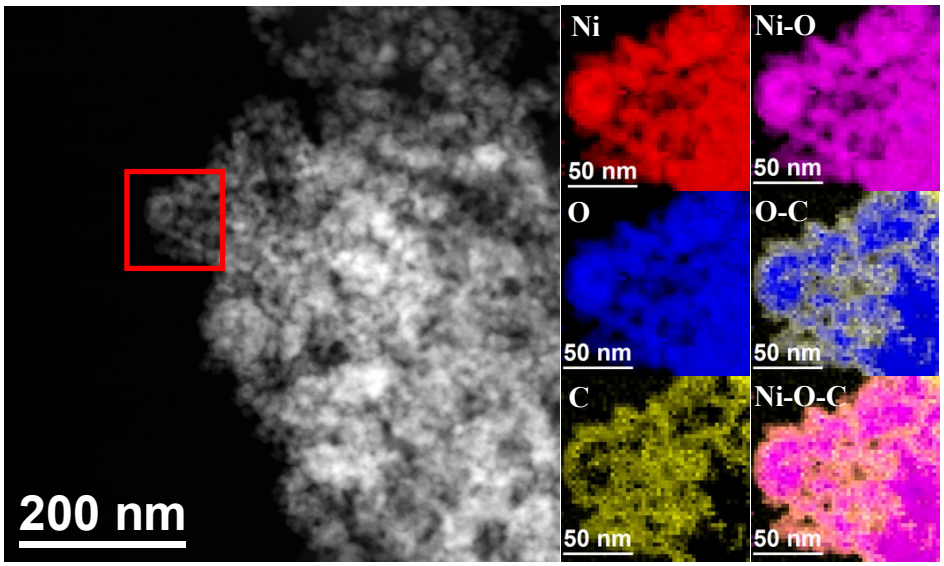

Figure S5. EELS chemical composition maps of NiNP@C from the area marked by the red square on the STEM micrograph. Individual Ni $L_{2,3}$-edges at 855 eV (red), O K-edge at 532 eV (blue) and C K-edge at 284 eV (yellow) as well as the composite (O-C and Ni-O-C) elemental maps.

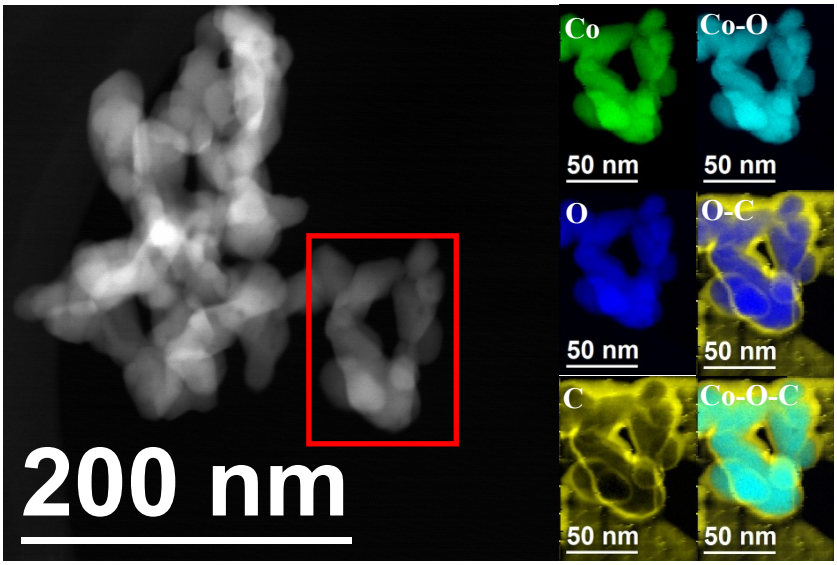

Figure S6. EELS chemical composition maps of CoNP@C from the area marked by the red square on the STEM micrograph. Individual Co $L_{2,3}$-edges at 779 eV (green), O K-edge at 532 eV (blue) and C K-edge at 284 eV (yellow) as well as the composite (O-C and Co-O-C) elemental map.

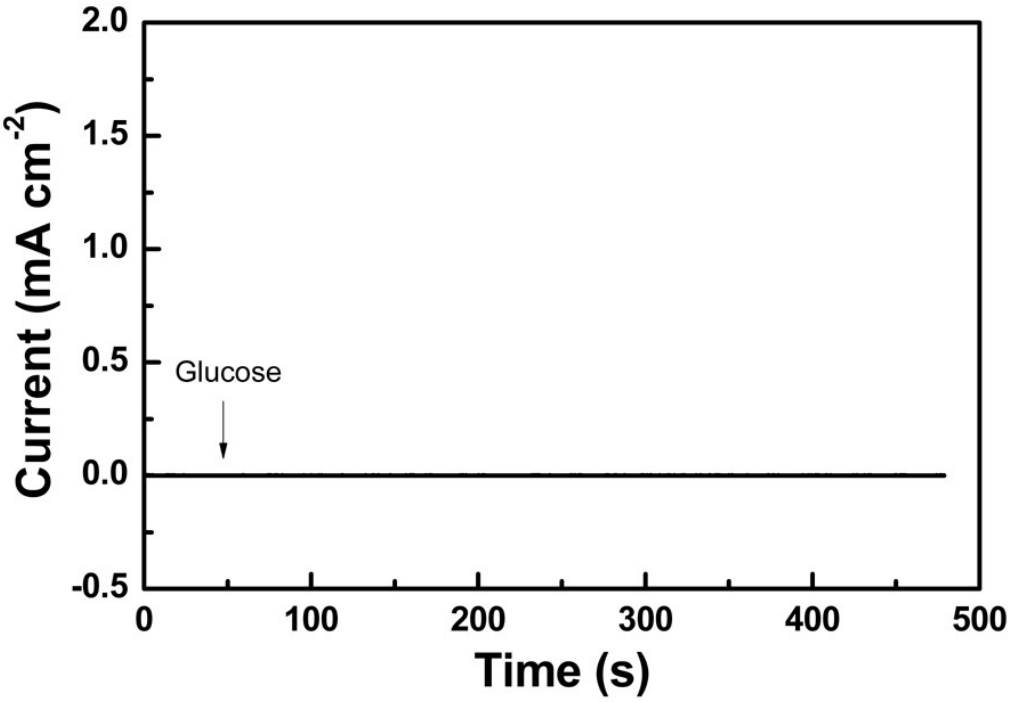

Figure S7. Amperometric response of carbon paper to the addition of 1 mM glucose at +0.55 V vs Hg/HgO to a solution of 0.1 M NaOH.

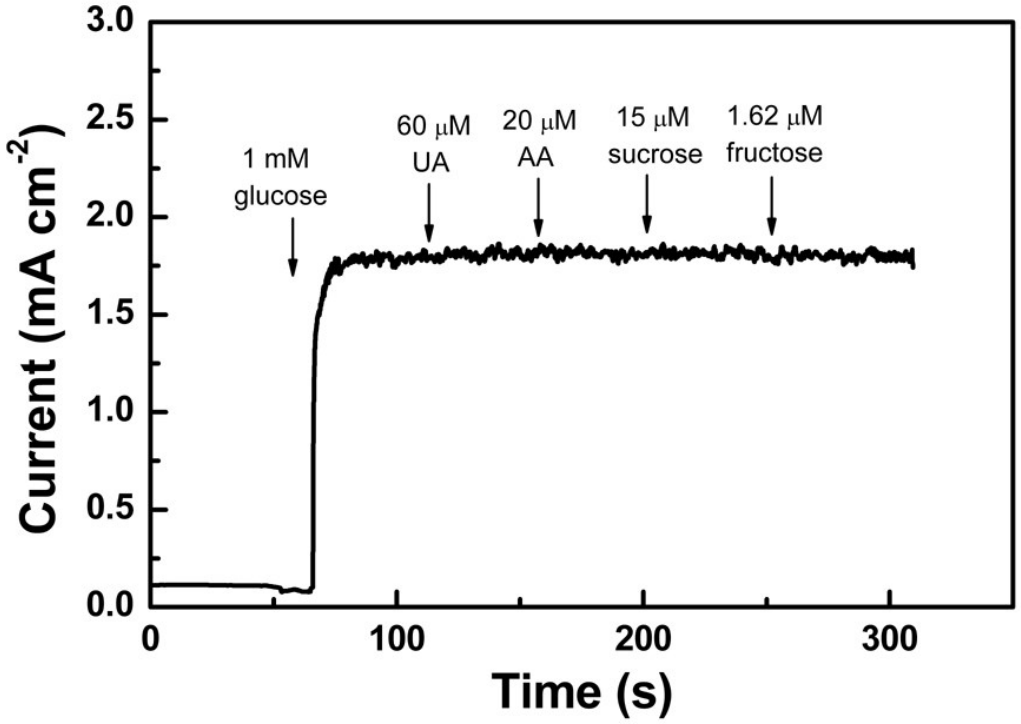

Figure S8. Amperometric response of YASNiCo@C catalyst coated on carbon paper after the addition of 1 mM of glucose and different concentrations of interferences at an applied potential of +0.55 V vs Hg/HgO to a solution of 0.1 M NaOH.

Table S8. Comparison of the sensitivity of YASNiCo@C electrode with other electrodes reported in literatures.

Ref.	Catalyst	Sensitivity ($\mu A\ cm^{-2}\ mM^{-1}$)	linear range (μM)	applied potential (V)	limit of detection (μM)	electrolyte
		Cobalt oxide				
S1	Co_3O_4 nanostructures	246.8	0.5–1000	0.54	0.012	0.1 M NaOH
S2	Cobalt nitride (Co_4N)	1137.2	600–10000	0.55	0.1	0.1 M NaOH
S3	Cobalt nitride nanosheets	921.18	10–8000	0.55	0.1	0.1 M NaOH
S4	Mesoporous Co_3O_4 Nanobundle	88	0.6-160	0.58	0.6	0.1 M NaOH
S5	Co-CoO-Co_3O_4 nanocomposites	949.3	5-600	0.55	0.92	0.1 M KOH
S6	Cobalt oxide nanoflowers	693.02	5-60	0.60	0.04	0.01M NaOH
S7	3D/Co_3O_4 thorn-like nanostructures	180	1-1000	0.55	0.046	0.1 M NaOH
S8	3D hierarchical porous Co_3O_4 film	366.03	1-500	0.60	1	0.1 M NaOH
S9	Porous CoOOH nanosheet	526.8	3-1109	0.52	1.37	0.1 M NaOH
S10	Nanoporous cobalt oxide nanowires	300.8	5-570	0.60	5	0.3 M NaOH
S11	Co_3O_4 nanoparticles	471.5	1-300	0.59	0.1	0.1 M NaOH
S12	CoNPs/ITO	1720	5-180	0.59	0.25	1 M NaOH
		Nickel oxide				
S13	Sandpaper-supported nickel coatings	1163.3	10-4300	0.60	0.25	0.1 M NaOH
S14	Ni layers modifie dboron-dope ddiamon	839.3	10-5640	0.40	1.23	1 M NaOH
S15	Nanostructured NiO electrode	206.9	100-10000	0.55	1.16	0.5 M NaOH
S16	$Ni(OH)_2$/PGE	948	4-3500	0.57	2	0.1 M NaOH
S17	Nf-$Ni(OH)_2$@oPPyNW	1049.2	1-4863	0.54	0.3	0.1 M NaOH
S18	NiO nanostructures	1915	100-5000	0.48	0.7	0.1 M NaOH
S19	Hedgehog-like NiO nanostructures	1052.8	500-4500	0.49	1.2	0.1 M NaOH
S20	NiO nanosheets	36.13	up to 10000	0.50	0.9	0.5 M NaOH
S21	Macro-mesoporous $Ni(OH)_2$	243	10-8300	0.50	1	0.1 M NaOH
		Cobalt-Nickel bimetallic oxide				
S22	Ni-Co Layered Double Hydroxide	292.84	5-50	0.55	0.8	0.1 M NaOH
S23	$NiCo_2O_4$ nanowires	72.4	0.37-2000	0.44	0.37	0.1 M NaOH
S24	$NiCo_2O_4$ hollow nanospheres	1917	10-300	0.55	0.6	0.2 M NaOH
S25	$NiCo_2O_4$ hollow nanorods	1685.1	3-1000	0.60	0.16	0.1 M NaOH
S26	Ni-Co bimetal nanowires	695	5-10000	0.45.	1.2	0.1 M NaOH
S27	NiCo-LDH	1235	5-1200	0.50	1.6	0.1 M NaOH
S28	Ni–Co alloy nanostructures	536.2	1-5000	0.50	0.39	0.1 M NaOH
		MOF-derived metal oxide				
S29	CuO nanorod	1523.5	up to 1250	0.60	1	0.1 M NaOH
S30	GS@ZIF-67 hybrids	1521.1	1-805.5	0.55	0.36	0.1 M NaOH
S31	Cu Nanospheres@Porous carbon	28.67	0.15-5620	0.45	0.48	0.1 M NaOH
S32	Cu-based structures	1255	3.76-1400	0.50	3.76	0.1 M NaOH
S33	Co nanoparticles with porous carbon	227	100-1100	0.50	5.69	0.1 M NaOH
S34	CuO/NiO-Carbon Nanocomposite	586.7	0.1-4500	0.65	0.037	0.1 M NaOH
S35	NiCo LDH nanosheets/graphene	344	5-800	0.60	0.6	0.1 M NaOH
This	YASNiCo@C	1964	5-1000	0.55	0.75	0.1 M NaOH

References:

S1. J. N. Xu, F. H. Li, D. D. Wang, M. H. Nawaz, Q. B. An, D. X. Han and L. Niu, Biosensors &

Bioelectronics, 2019, 123, 25-29.
S2. T. T. Liu, M. A. Li and L. P. Guo, Talanta, 2018, 181, 154-164.
S3. T. T. Liu, M. Li, P. Dong, Y. J. Zhang and L. P. Guo, Sensors and Actuators B-Chemical, 2018, 255, 1983-1994.
S4. A. V. N. Kumar, Y. H. Li, S. L. Yin, C. J. Li, H. R. Xue, Y. Xu, X. N. Li, H. J. Wang and L. Wang, Chem-Asian J, 2018, 13, 2093-2100.
S5. J. Yu, Y. H. Ni and M. H. Zhai, Journal of Alloys and Compounds, 2017, 723, 904-911.
S6. S. Mondal, R. Madhuri and P. K. Sharma, J Mater Chem C, 2017, 5, 6497-6505.
S7. P. Kannan, T. Maiyalagan, E. Marsili, S. Ghosh, L. H. Guo, Y. J. Huang, J. A. Rather, D. Thiruppathi, J. Niedziolka-Jonsson and M. Jonsson-Niedziolka, Analyst, 2017, 142, 4299-4307.
S8. S. S. Fan, M. G. Zhao, L. J. Ding, J. J. Liang, J. Chen, Y. C. Li and S. G. Chen, Journal of Electroanalytical Chemistry, 2016, 775, 52-57.
S9. L. Zhang, C. L. Yang, G. Y. Zhao, J. S. Mu and Y. Wang, Sensors and Actuators B-Chemical, 2015, 210, 190-196.
S10. L. Q. Kang, D. P. He, L. L. Bie and P. Jiang, Sensors and Actuators B-Chemical, 2015, 220, 888-894.
S11. L. Han, D. P. Yang and A. H. Liu, Biosensors & Bioelectronics, 2015, 63, 145-152.
S12. T. Wang, Y. A. Yu, H. F. Tian and J. B. Hu, Electroanalysis, 2014, 26, 2693-2700.
S13. Y. M. Xu, L. Hou, H. Zhao, S. Y. Bi, L. Zhu and Y. X. Lu, Applied Surface Science, 2019, 463, 1028-1036.
S14. H. Y. Long, X. Z. Liu, Y. N. Xie, N. X. Hu, Z. J. Deng, Y. L. Jiang, Q. P. Wei, Z. M. Yu and S. G. Zhang, Journal of Electroanalytical Chemistry, 2019, 832, 353-360.
S15. C. Heyser, R. Schrebler and P. Grez, Journal of Electroanalytical Chemistry, 2019, 832, 189-195.
S16. M. L. Chelaghmia, M. Nacef, A. M. Affoune, M. Pontie and T. Derabla, Electroanalysis, 2018, 30, 1117-1124.
S17. J. Yang, M. Cho, C. Pang and Y. Lee, Sensors and Actuators B-Chemical, 2015, 211, 93-101.
S18. R. A. Soomro, Z. H. Ibupoto, Sirajuddin, M. I. Abro and M. Willander, Journal of Solid State Electrochemistry, 2015, 19, 913-922.
S19. R. A. Soomro, Z. H. Ibupoto, Sirajuddin, M. I. Abro and M. Willander, Sensors and Actuators B-Chemical, 2015, 209, 966-974.
S20. H. Liu, X. L. Wu, B. Yang, Z. J. Li, L. C. Lei and X. W. Zhang, Electrochimica Acta, 2015, 174, 745-752.
S21. Y. Fan, Z. J. Yang, X. H. Cao, P. F. Liu, S. Chen and Z. Cao, Journal of the Electrochemical Society, 2014, 161, B201-B206.
S22. Y. J. Gao, Q. H. Yu, Y. T. Du, M. Yang, L. Gao, S. Q. Rao, Z. Q. Yang, Q. C. Lan and Z. J. Yang, Journal of Electroanalytical Chemistry, 2019, 838, 41-47.
S22. G. Ni, J. Cheng, X. Dai, Z. H. Guo, X. Ling, T. Yu and Z. J. Sun, Electroanalysis, 2018, 30, 2366-2373.
S23. Z. H. Qin, Q. P. Cheng, Y. Lu and J. F. Li, Applied Physics a-Materials Science & Processing, 2017, 123.
S24. W. Huang, Y. Cao, Y. Chen, J. Peng, X. Y. Lai and J. C. Tu, Applied Surface Science, 2017, 396, 804-811.
S25. J. Yang, M. Cho and Y. Lee, Biosensors & Bioelectronics, 2016, 75, 15-22.
S26. K. Ramachandran, T. R. Kumar, K. J. Babu and G. G. Kumar, Scientific Reports, 2016, 6.
S27. J. Chen, Q. L. Sheng, Y. Wang and J. B. Zheng, Electroanalysis, 2016, 28, 979-984.

S28. M. Ranjani, Y. Sathishkumar, Y. S. Lee, D. J. Yoo, A. R. Kim and G. G. Kumar, Rsc Advances, 2015, 5, 57804-57814.
S29. K. Kim, S. Kim, H. N. Lee, Y. M. Park, Y. S. Bae and H. J. Kim, Applied Surface Science, 2019, 479, 720-726.
S30. X. R. Chen, D. Lau, G. J. Cao, Y. Tang and C. Wu, Acs Appl Mater Inter, 2019, 11, 9374-9384.
S31. Y. Xie, Y. H. Song, Y. Y. Zhang, L. J. Xu, L. F. Miao, C. W. Peng and L. Wang, Journal of Alloys and Compounds, 2018, 757, 105-111.
S32. L. B. Shi, X. H. Niu, H. L. Zhao and M. B. Lan, Chemelectrochem, 2017, 4, 246-251.
S33. L. B. Shi, Y. F. Li, X. Cai, H. L. Zhao and M. B. Lan, Journal of Electroanalytical Chemistry, 2017, 799, 512-518.
S34. V. Archana, Y. Xia, R. Y. Fang and G. G. Kumar, Acs Sustain Chem Eng, 2019, 7, 6707-6719.
S35. E. Asadian, S. Shahrokhian and A. I. Zad, Journal of Electroanalytical Chemistry, 2018, 808, 114-123.